Contents lists available at ScienceDirect

Heliyon

Heliyon

Research Article

High fat diet modulates the protein content of nutrient transporters in the small intestine of mice: possible involvement of PKA and PKC activity

Andressa Harumi Torelli Hijo [a], Camille Perella Coutinho [a], Tatiana Carolina Alba-Loureiro [a], Jaqueline Santos Moreira Leite [a], Paula Bargi-Souza [b], Francemilson Goulart-Silva [a,*]

[a] Department of Physiology and Biophysics, Institute of Biomedical Sciences, University of São Paulo, Brazil
[b] Department of Physiology and Biophysics, Institute of Biological Science, Federal University of Minas Gerais, Brazil

ARTICLE INFO

ABSTRACT

Aims: Chronic high fat consumption has been shown to modulate nutrient transporter content in the intestine of obese mice; however it is unclear if this regulation occurs before or after the establishment of obesity, and the underlying molecular mechanism requires elucidation.

Main methods: Towards this goal C57BL/6 mice were fed a low fat diet (LFD) or high fat diet (HFD), and specific protein and gene expression levels were assessed for up to 12 weeks. Similar experiments were also performed with leptin-deficient (Ob/Ob) mice.

Key findings: The results showed that the HFD group presented decreased GLUT2, PEPT1, FAT/CD36 and NPC1L1, and increased NHE3, MTTP and L-FABP content. Animals fed an HFD also presented enhanced lipid transporter gene expression of Slc27a4, Npc1l1, Cd36, Mttp and L-Fabp. Additionally, FAT/CD36 and NPC1L1 protein levels were reduced in both HFD-induced obese and Ob/Ob mice. Ob/Ob mice also exhibited increased Slc2a2 and Slc15a1 mRNAs expression, but the protein expression levels remained unchanged. The HFD also attenuated PKA and PKC activities. The inhibition of PKA was associated with decreased FAT/CD36 content, whereas increased L-FABP levels likely depend on CREB activation, independent of PKA. It is plausible that the HFD-induced changes in NPC1L1, MTTP and L-FABP protein content involve regulation at the level of transcription. Moreover, the changes in GLUT2 and PEPT1 content might be associated with low PKC activity.

Significance: The results indicated that an HFD is capable of reducing nutrient transporter content, possibly attenuating nutrient uptake into the intestine, and may represent a feedback mechanism for regulating body weight. Furthermore, the elevated levels of NHE3, L-FABP and MTTP may account for the increased prevalence of hypertension and dyslipidemia in obese individuals. All of these changes are potentially linked to reduced PKA or PKC activities.

1. Introduction

The products of macronutrient digestion are absorbed by the intestinal epithelium, through specific nutrient transporters located on the apical side of the enterocyte membrane. The absorption of carbohydrates is mediated by Sodium-Coupled Glucose Transporter -1 (SGLT1), Glucose Transporters -2 (GLUT2) and -5 (GLUT5) [1], whereas the uptake of peptides is facilitated by Peptide Transporter -1 (PEPT1), which depends on Sodium/Hydrogen Exchanger (NHE) activity, mainly NHE3 [2]. Additionally, it is known that lipid transport involves fatty acid transporter protein -4 (FATP4) and fatty acid translocase (FAT/CD36), for long chain fatty acid uptake, and that cholesterol endocytosis is mediated

by Niemann-Pick C1-like 1 (NPC1L1) [3].

The regulation of these nutrient transporters in the lumen of the gastrointestinal (GI) tract is poorly understood and could involve nutrients themselves. In fact, our group previously reported that hypo- and hyperthyroid mice fed a high fat diet (HFD), for 16 weeks, exhibited a significant decrease in the expression of GLUT2, PEPT1, FAT/CD36 and NPC1L1, in the small intestine [4], which, as a consequence, could impair nutrient uptake in these animals.

High fat intake leads to elevated fat levels in the enterocytes [5], which could modulate the expression of nutrient transporters and possibly interfere with intracellular lipid processing. In support of these potential consequences, previous studies have demonstrated the

---

* Corresponding author.
  E-mail addresses: goulart@icb.usp.br, goufran@hotmail.com (F. Goulart-Silva).

presence of dyslipidemia in HFD-induced obese mice, as well as in leptin-deficient (Ob/Ob) mice [6, 7]. Additionally, modulating the expression levels of liver fatty-acid binding protein (L-FABP) and microsomal triglyceride transfer protein (MTTP), which are responsible for the transport of fatty acids from the cytosol to the endoplasmic reticulum and the incorporation of lipids into pre-chylomicrons, respectively, could directly affect the amount of chylomicrons secreted into the lymph, and consequently into the bloodstream [8, 9, 10]. Furthermore, previous studies showed that the gene expression levels of *Fabp1* and *Mttp* were downregulated in the livers of animals fed an HFD [11, 12, 13, 14].

However, it is unclear whether the observed alterations in the intestinal nutrient transporter expression are a consequence of the HFD or due to the obesity, itself, since HFD-induced obese and Ob/Ob mice display similar endocrine and metabolic disorders, including the aforementioned dyslipidemia, as well as hypertension and cardiovascular diseases [15, 16, 17].

With regards to possible molecular mechanisms triggered by an HFD and diminished nutrient transporter expression and/or activity, protein kinases A (PKA) and C (PKC) represent potential targets. For example, previous studies have shown that an HFD can modulate the activity and protein levels of these protein kinases in the hypothalamus, muscle and liver [18, 19, 20]. Thus, it is plausible that an HFD could regulate the activities of PKA and PKC in the small intestine, thus perturbing enterocyte physiology, by affecting nutrient uptake and lipid processing.

Thus, the present study sought to determine if a correlation exists among the high fat intake, the reduced intestinal nutrient transporter expression and the PKA and PKC activities, as well as, to elucidate the molecular mechanism underlying the HFD-mediated modulation of nutrient uptake and the subsequent impact on enterocyte physiology.

2. Materials and methods

2.1. Animals and treatment

All of the procedures performed in this study were approved by Ethical Committee on Animal Use at the University of São Paulo (numbers 106/2014, 134/2015 and 99/2017). Wild-type adult male C57BL/6 mice were obtained from the Animal Facility at the University of São Paulo Faculty of Medicine and received either a standard low fat diet (LFD) or high fat diet (HFD) from the second month of age until the day of their euthanasia, which occurred 3, 6, 9 or 12 weeks after initiating the diet. The rodent chows were purchased from PragSoluções (Brazil). Tables providing all of the ingredients of diets (LFD and HFD) as well as fatty acids composition are exactly as published previously [21, 22]. In summary, LFD contained 70% carbohydrate, 20% protein and 10% lipid, and the HFD contained 20% carbohydrate, 20% protein and 60% lipid. Adult five-month-old male mice fed the LFD were also injected with H89 (20 mg/Kg) (Sigma-Aldrich, Inc., USA) subcutaneous every 8 h for 24 h [23].

The genetically obese Ob/Ob mice were obtained from Jackson Laboratories (000632 B6.Cg-Lepob/J, Bar Harbor, ME), and were used to compare the evaluated parameters with the wild-type C57BL/6 mice. These mice were fed commercial chow (NUVILAB CR1, Nuvital Nutrientes LTDA, Brazil) and euthanized at five months of age. All the animals were maintained under a 12 h light/dark cycle (lights on at 6:00 am), in a temperature controlled room (22 ± 2 °C), with a relative humidity of $55 \pm 15\%$ and provided with water and chow *ad libitum*.

Mice were euthanized by decapitation under isoflurane inhalation anaesthesia, and the small intestines were removed, inverted and washed with saline to remove luminal content. The epithelium was then isolated from the mucosa, as previously described [4].

2.2. Western blotting

The mucosal epithelium was removed, transferred to lysis buffer (150 mM NaCl, 0.5% sodium deoxycholate, 50 mM Tris·HCl, pH 8, 0.1% SDS, 0.1% Nonidet P-40, 2 mM Na_3VO_4, 10 mM NaF, 0.2 mM phenylmethylsulfonyl fluoride (PMSF) supplemented with protease inhibitors (Roche Diagnostics)) [24], homogenized with a motorized tissue grinder (Fisher Scientific, Inc., USA) and frozen at -80 °C until the day of protein processing. After thawing, the homogenate was centrifuged at $17,949 \times g$ for 20 min at 4 °C (Centrifuge 5804R, Eppendorf, Germany) and the supernatant was collected.

The protein concentration of the supernatant was determined using the Bradford assay [25] and 90 μg of total protein per sample was heated at 37 °C for 30 min, and then subjected to SDS-PAGE. Protein molecular weights were estimated using protein markers (ACTGene, Inc., USA). The proteins were then transferred to nitrocellulose membranes (Bio-Rad Laboratories, Inc., USA), stained with Ponceau S, to assess transfer efficiency, scanned and blocked with 5% skimmed milk at room temperature (RT) for 1 h.

The membranes were incubated with the target protein specific primary antibody at 4 °C, overnight. All primary antibodies were purchased from Santa Cruz Biotechnology, Inc., USA, with the exception of SGLT1, GLUT5, MTTP and CREB antibodies, which were obtained from Merck Millipore, Inc., USA, GeneTex, Inc., USA, LifeSpan BioScience, Inc., USA, and Cell Signaling Technology, Inc., USA, respectively. The membranes were washed and incubated with the appropriate peroxidase-conjugated secondary antibody (Jackson Immunoresearch laboratories, Inc., USA), according to the host species of the primary antibodies, for 75 min at RT.

After washing, the blots were developed and the target proteins were detected by Enhanced Chemiluminescent (ECL). Images of the bands were captured using an Amersham Imager 600 photodocumentation system (GE Healthcare Company, UK) and analyzed with the Image J software (National Institute of Health, USA). The Ponceau S images were used for the normalization of the protein quantity detected on the immunoblots [26], and are shown in Supplementary data 1.

2.3. Enzyme-linked immunosorbent assay (ELISA)

The epithelium isolated from intestinal mucosa was homogenized in

Table 1
RT-qPCR primer sequences.

| Gene	Gene Bank #	Foward sequence	Reverse sequence
18s	NR_003278.3	GCGAATGGCTCATTAAATCAGTTA	TGGTTTTGATCTGATAAATGCACG
Cd36	NM_001159558.1	GCTAAATGAGACTGGGACCAT	CACCACTCCAATCCCAAGTAA
Slc15a1	NM_053079.2	CAAACAGTGGGCTGAGTACA	GCTGGGTTGATGTAGGTGTAG
Slc9a3	NM_001081060.1	GCAGGAGTACAAGCATCTCT	TCCATAGGCAGTTTCCCATTAG
Npc1l1	NM_207242.2	CCAGATTATAGCCTCCCAGTTC	CCGTAGTTCAGCTGTGATGT
Slc2a2	NM_031197.2	TCTGTCTGTGTCCAGCTTTG	CCAACATTGCTTTGATCCTTCC
Slc2a5	NM_019741.3	GGTTGGAATCTGTGCAGGTAT	GCCGACAGTGATGAAGAGTT
Slc5a1	NM_019810.4	AGTGGGCAGCTCTTTGATTAC	CCAGAAGGCTCCTTGTTCATT
Slc27a4	NM_011989.4	GTGGTGCACAGCAGGTATTA	GTTTCCTGCTGAGTGGTAGAG
L-Fabp	NM_017399.4	AGGGGGTGTCAGAAATCGTG	CCCCCAGGGTGAACTCATTG
Mttp	NM_001163457.2	AGACCCCTAAGCTCGTTTTCT	TTTGCTTGGGGTTCCTTTCACC
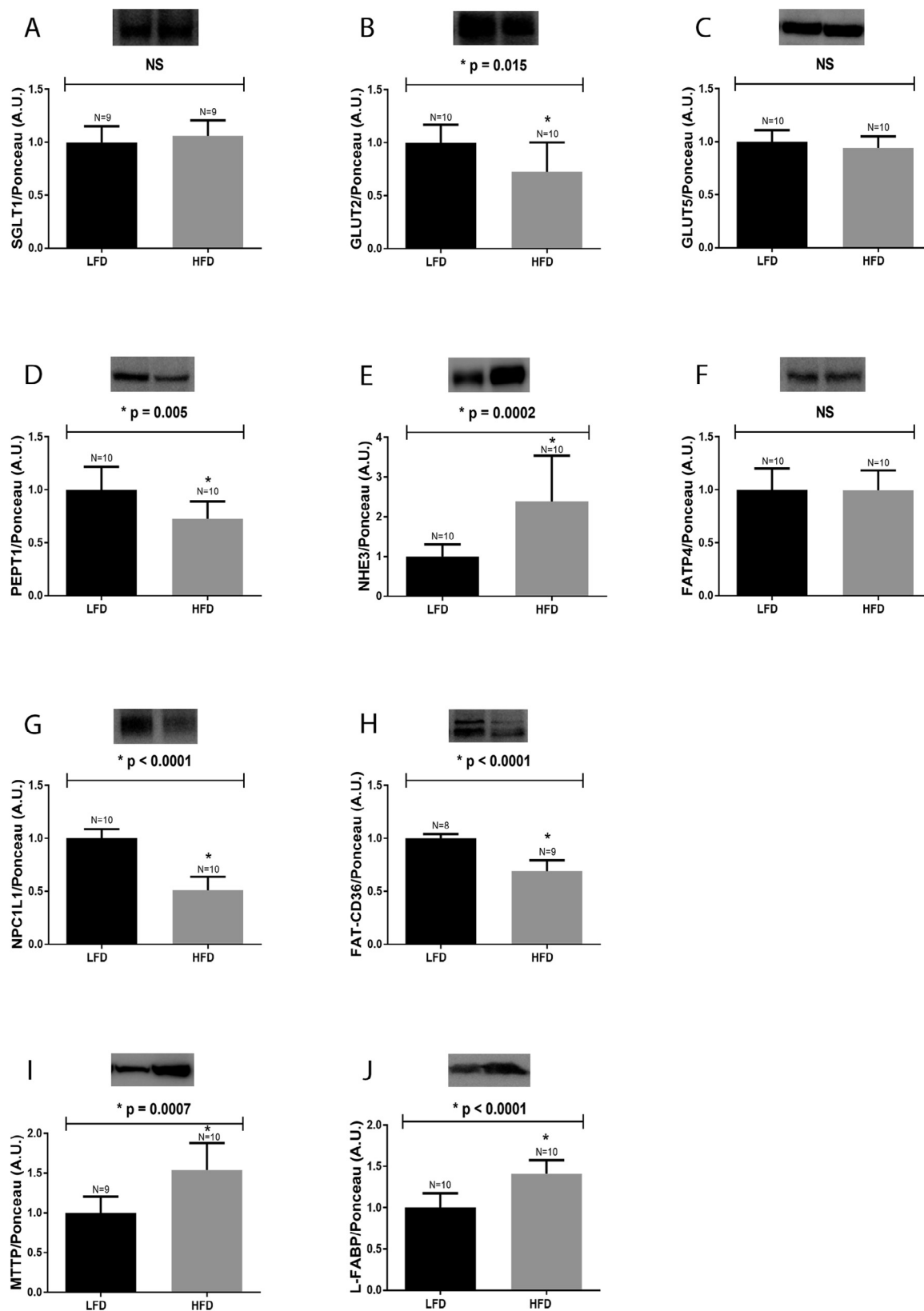
Fig. 1. Protein expression in the small intestine of mice fed a HFD. Mice fed an HFD for 12 weeks were euthanized, and the intestinal epithelium was removed, homogenized and processed for detecting the followings proteins: A: SGLT1, B: GLUT2, C: GLUT5, D: PEPT1, E: NHE3, F: FATP4, G: NPC1L1, H: FAT-CD36, I: MTTP and J: L-FABP. Representative blots are displayed at the top of each graph. The number of animals analyzed for each group (N) is also displayed above each bar. Densitometry was used to measure the intensity of each band, and these values, expressed in arbitrary units (A.U.), were normalized by Ponceau-S staining intensity. The results were analyzed using the Student's "t" test. NHE3 data (E) was subjected to the non-parametric test, and all of the other proteins were evaluated using the parametric test. The p values of statistically significant results are presented above the bars of the graph; non-significant (NS) data are also indicated. The nitrocellulose membrane was cut at the level of the target proteins using a standard molecular marker as guide. The full area of the selected blots is shown in supplementary data 2.
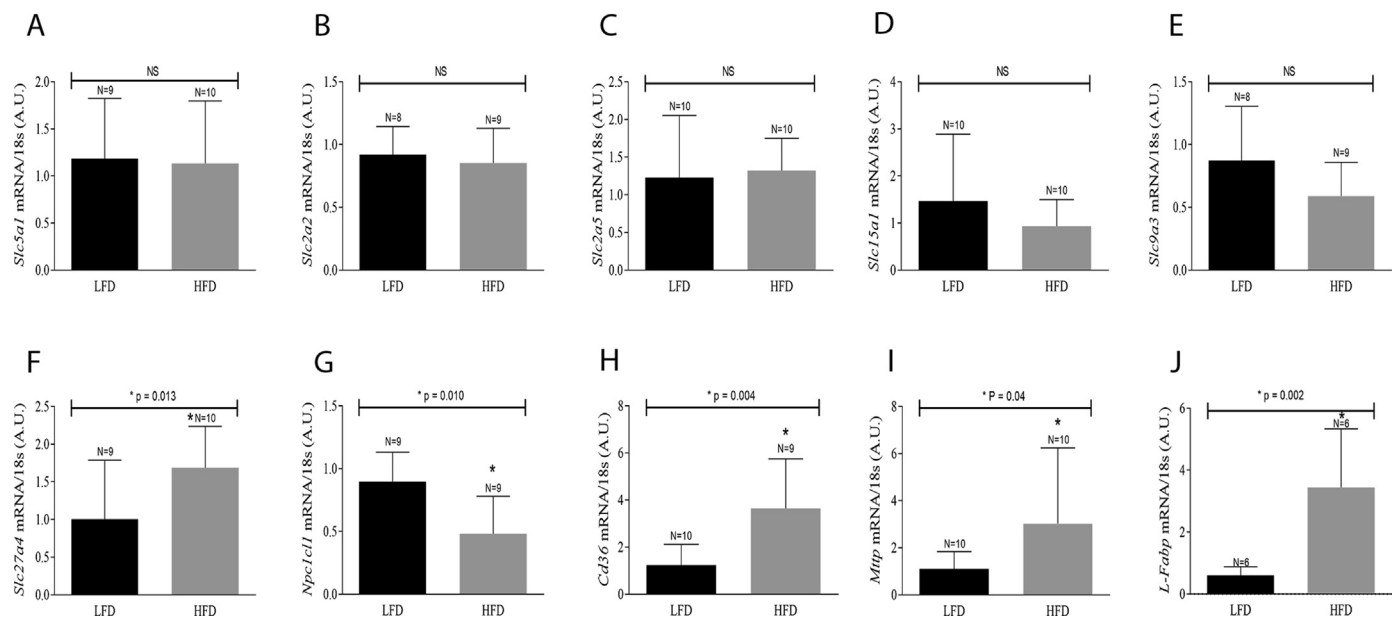
Fig. 2. mRNA expression in the small intestine of mice fed a HFD. Mice fed either LFD or HFD were euthanized after 12 weeks. The intestinal epithelium was removed, homogenized and submitted to RT-qPCR. The values obtained for each target gene were normalized with the expression levels of the housekeeping gene 18s and evaluated using Student's t test. *Slc5a1* [SGLT1], *Slc2a2* [GLUT2], *Slc9a3* [NHE3] and *Cd36* [FAT/CD36] were subjected to a parametric test, while *Slc2a5* [GLUT5], *Slc15a1* [PEPT1], *Slc27a4* [FATP4], *Npc1l1* [NPC1L1], *Mttp* [MTTP] and *L-Fabp* [L-FABP] were subjected to a non-parametric test. "N" represents the number of animals/group. The p values of statistically significant results are presented above the bars of the graph; non-significant (NS) data are also indicated.

the same lysis buffer used for immunoblotting. Total protein content was quantified using the Bradford assay. Twenty μg of total protein was applied to each sample well of the microtiter plate. The procedures were carried out according to the instructions of the manufacturer, and absorbance was detected at 450 nm, with a SpectraMax-M5 absorbance spectrophotometer (Molecular devices, USA). Relative kinase activity rates were calculated according to the instructions of the manufacturer. The data were expressed as PKA or PKC relative activities per 20 μg of total intestinal epithelium protein.

2.4. Real time qPCR

The intestinal epithelium was lysed, and the total RNA was extracted, according to the Trizol® reagent protocol, and treated with DNase (Ambion RNA by Life Technologies/Invitrogen). Reverse transcription (RT) was carried out using one microgram of total RNA and a random primer (Invitrogen®), using the M-MLV Reverse Transcriptase (Promega®, USA). The RT product was diluted according to the efficiency curve and submitted to real-time quantitative PCR (RT-qPCR) using the Platinum SYBR Green quantitative PCR Super Mix UDG (Invitrogen®).

The specific primer sequences used are provided in Table 1. PCR reactions were performed in a Corbett RotorGene system (Corbett Life Sciences, Australia) under the following conditions: 40 cycles at 95 °C for 15 s, 60 °C for 15 s, and 72 °C for 30 s and the Melting Curve was performed from 65 °C up to 97 °C for 1 min. The Ct values were recorded for each gene, and normalized using the results obtained with the housekeeping gene *18s*, which was selected using the geNorm software. The results were calculated according to the $2^{-\Delta\Delta CT}$ method [27, 28, 29, 30].

2.5. Statistical analysis

The data are presented as the mean ± standard deviation (SD) of 1–3 independent experiments, which were submitted either the Student's t-test or a two-way ANOVA using the GraphPad Prism 7.04 software. Differences were considered significant at p < 0.05. A parametric test

was applied to data with a normal distribution of probability and homogeneity of variance. A non-parametric test was applied to data that failed to meet these criteria. The statistical tests utilized and the number of animals (N) evaluated are described in the figure legends.

3. Results

3.1. Analysis of nutrient transporter expression in mice fed an HFD

After being fed the HFD for 12 weeks, the protein expression levels of SGLT1, GLUT5, GLUT2, PEPT1, FATP4, FAT-CD36, NPC1L1, NHE3, MTTP and L-FABP in the small intestine of mice were evaluated. As presented in Fig. 1, the levels of GLUT2 (Fig. 1, Panel B), PEPT1 (Fig. 1, Panel D), FAT/CD36 (Fig. 1, Panel H) and NPC1L1 (Fig. 1, Panel G) were reduced in mice fed the HFD, when compared to LFD controls. On the contrary, there was observed an increase in NHE3 (Fig. 1, Panel E), MTTP (Fig. 1, Panel I) and L-FABP (Fig. 1, Panel J) expression in the small intestine of the HFD group, when compared to the control mice. The protein expression levels of SGLT1 (Fig. 1, Panel A), GLUT5 (Fig. 1, Panel C) and FATP4 (Fig. 1, Panel F) were not affected by high fat intake.

To determine the level (transcriptionally or translationally) nutrient transporter expression is regulated, lipid transporter mRNAs were analyzed by RTq-PCR, in animals fed an HFD for 12 weeks. There was an observed upregulation in the expression of *Slc27a4* (Fig. 2, Panel F), *Cd36* (Fig. 2, Panel H), *Mttp* (Fig. 2, Panel I) and *L-Fabp* (Fig. 2, Panel J), while *Npc1l1* expression was found to be downregulated (Fig. 2, Panel G), in the intestine of mice fed HFD. These mRNA transcripts encode for lipid transporters FATP4, FAT/CD36, MTTP, L-FABP and NPC1L1, respectively. Additionally, the expression of *Slc5a1* (Fig. 2, Panel A), *Slc2a2* (Fig. 2, Panel B), *Slc2a5* (Fig. 2, Panel C), *Slc15a1* (Fig. 2, Panel D) and *Slc9a3* (Fig. 2, Panel E), which correspond to SGLT1, GLUT2, GLUT5, PEPT1 and NHE3, respectively, remained unchanged after 12 weeks of a HFD diet. Thus, the observed HFD-induced changes in NPC1L1, MTTP and L-FAPB protein expression appeared to be transcriptionally regulated.
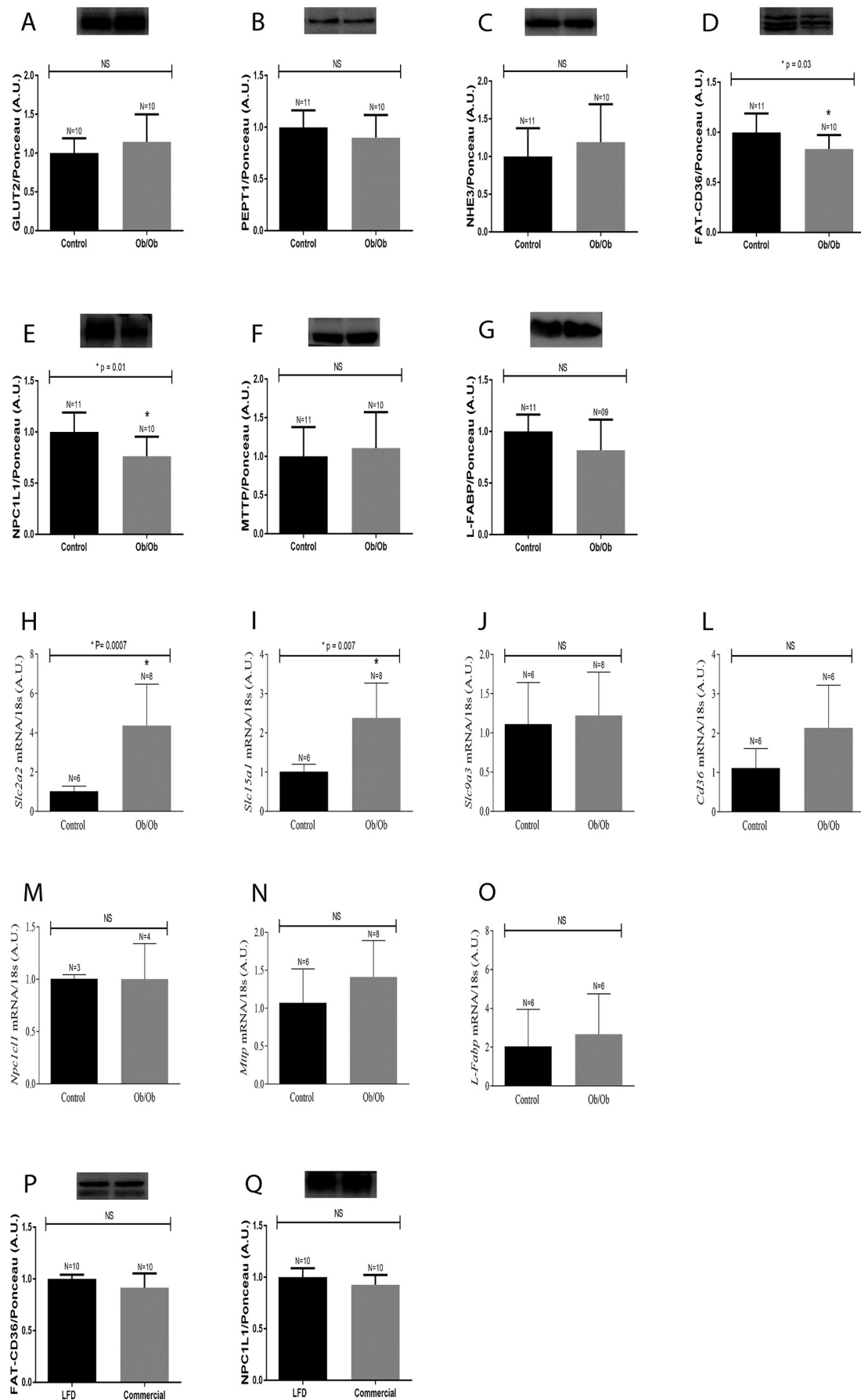
(caption on next page)

Fig. 3. Protein and mRNA expression in the small intestine of Ob/Ob mice. Five month old wild-type and Ob/Ob mice were euthanized, and the intestinal epithelium was removed, homogenized and processed for protein and mRNA expression: Panels A to G, as well as P and Q represent protein expression. Representative blots are displayed at the top of each graph. Densitometry was used to measure the intensity of each band, and these values, expressed in arbitrary units (A.U.), were normalized by Ponceau-S staining intensity. Panels H to O represent mRNA quantification as determined by RTq-PRC analyses. The number of animals analyzed for each group (N) is displayed above each bar. The results were analyzed using the Student's t-test and a non-parametric test was applied for NHE3 and MTTP protein content and for all the mRNAs evaluated. The remaining proteins were evaluated using a parametric test. The p values of statistically significant results are presented above the bars of the graph; non-significant (NS) data are also indicated. The nitrocellulose membrane was cut at the level of the target proteins using a standard molecular marker as guide. The full area of the selected blots is shown in supplementary data 2.
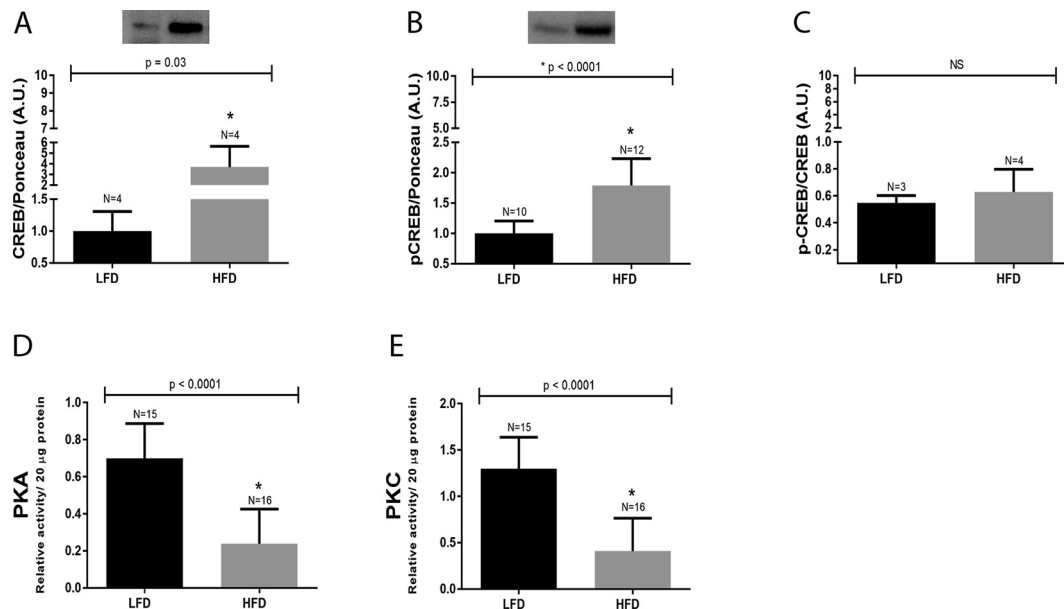

Fig. 4. CREB protein content and PKA/PKC activities in the small intestine of mice fed a HFD. Mice were euthanized at 12th week after being fed either a LFD or HFD. The intestinal epithelium was removed, homogenized and submitted to immunoblotting against total and phosphorylated CREB (4A and 4B) as well as pCREB/CREB ratio (4C), or used for kinases activities by ELISA (4D and 4E). The number of animals analyzed for each group (N) is displayed above each bar. A representative CREB blots are displayed at the top of each panel. The total and phosphorylated CREB densitometry was normalized by Ponceau-S staining intensity. The p values are presented above the bars of the graphs. The nitrocellulose membrane was cut at the level of the target proteins using a standard molecular marker as guide. The full area of the selected blots is shown in supplementary data 2.

3.2. Analysis of nutrient transporter content in Ob/Ob mice

A similar analysis of intestinal nutrient transporter expression was also carried out in genetically obese Ob/Ob mice, in an attempt to determine whether the observed alterations in protein content were related to the HFD or obesity, independent of cause. The leptin-deficient obese Ob/Ob mice exhibited a reduction in FAT/CD36 (Fig. 3, Panel D) and NPC1L1 (Fig. 3, Panel E) content, as noted in the HFD-induced obese mice. However, unlike the HFD obese animals, the levels of GLUT2 (Fig. 3, Panel A), PEPT1 (Fig. 3, Panel B), NHE3 (Fig. 3, Panel C), MTTP (Fig. 3, Panel F) and L-FABP (Fig. 3, Panel G) were not perturbed in the small intestine of Ob/Ob mice, when compared to control mice (Fig. 3 A-G).

We also analyzed the expression of nutrient transporter genes in the intestinal epithelium of Ob/Ob mice. This analysis revealed an upregulation in the expression of *Slc2a2* (Fig. 3, Panel H) and *Slc15a1* (Fig. 3, Panel I), while *Slc9a3* (Fig. 3, Panel J), *Cd36* (Fig. 3, Panel L), *Npc1l1* (Fig. 3, Panel M), *Mttp* (Fig. 3, Panel N) and *L-Fabp* (Fig. 3, Panel O) expression levels remained unchanged, when compared to control LFD fed mice. It is also worth pointing out that there was no correlation between the mRNA expression and the protein levels in Ob/Ob mice.

To rule out the possibility that the type of chow, commercial for the Ob/Ob and LFD for HFD-induced obesity controls, influenced these observed changes in protein expression, wild-type mice were fed the chow commercial, and the protein expression of FAT/CD36 and NPC1L1

were evaluated. The results showed no changes in the levels of FAT/CD36 (Fig. 3, Panel P) and NPC1L1 (Fig. 3, Panel Q).

3.3. Analysis of HFD on PKA and PKC activities and CREB content

Next the potential involvement of CREB (total and phosphorylated), PKA and PKC were evaluated in mice fed the HFD for 12 weeks. Total and phosphorylated CREB levels (Fig. 4, Panel A and Panel B) were found to be elevated in the small intestine of HFD-induced obese mice, when compared to the LFD mice. However, when phosphorylated CREB (pCREB) was normalized by total CREB we were unable to detect any difference between the LFD and HFD groups (Fig. 4, Panel C), which indicated that the elevated pCREB levels in HFD-group was a consequence of augmented total CREB content. On the other hand, the activities of PKA (Fig. 4, Panel D) and PKC (Fig. 4, Panel E) were significantly reduced in the small intestine of mice fed HFD, when compared to the LFD controls.

The discrepancy between PKA activity and pCREB protein was further evaluated, under the same experimental conditions, by administering the PKA inhibitor H89 to animals fed an LFD. In this experimental model, PKA inhibition by H89 was confirmed by a significant decrease in pCREB protein levels (Fig. 5, Panel A). Additionally, the protein content of FAT/CD36 (Fig. 5, Panel E) and L-FABP (Fig. 5, Panel H) were also reduced in the small intestine. However, the levels of GLUT2 (Fig. 5, Panel B), PEPT1 (Fig. 5, Panel C), NHE3 (Fig. 5, Panel D), NPC1L1 (Fig. 5, Panel F) and
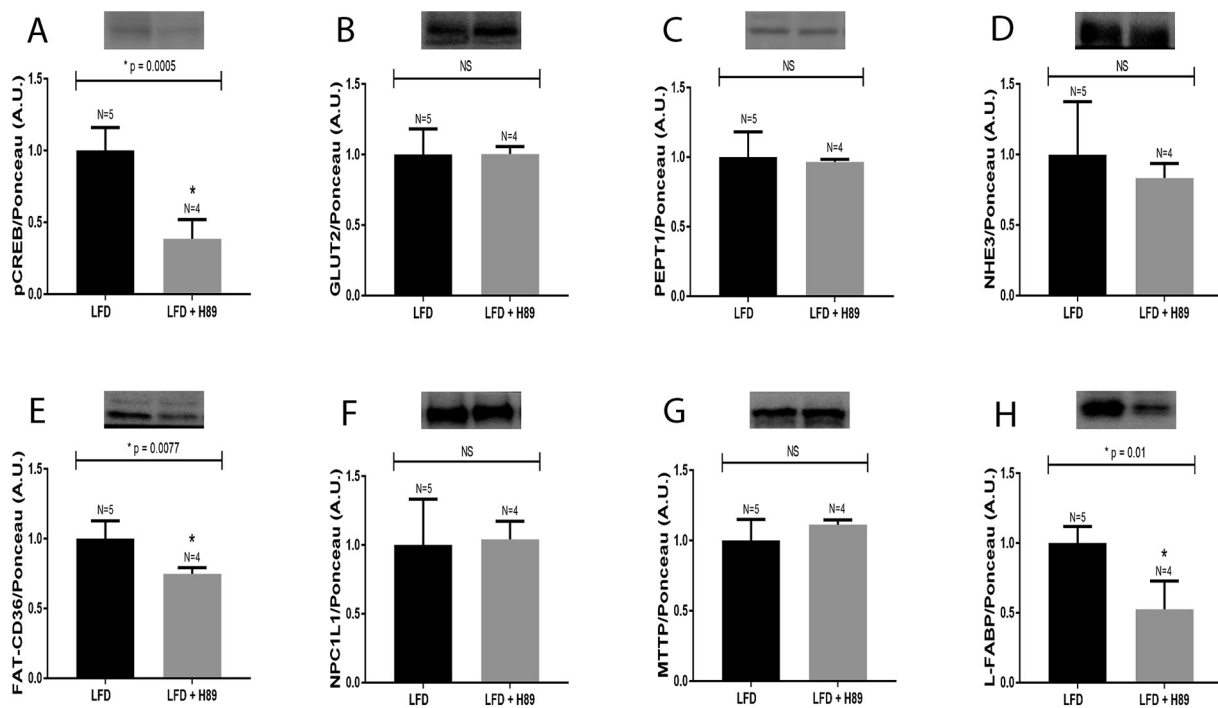
Fig. 5. Protein expression in the small intestine of mice treated with H89. Mice fed a LFD for 12 weeks were treated with H89 or vehicle (5% DMSO), every 8 h, for 24 h. Mice were then euthanized, and the intestinal epithelium was removed, homogenized and processed for detecting the followings proteins: A: pCREB, B: GLUT2, C: PEPT1, D: NHE3, E: FAT-CD36, F: NPC1L1, G: MTTP and H: L-FABP. Representative blots are displayed at the top of each graph. The number of animals analyzed for each group (N) is also displayed above each bar. Densitometry was used to measure the intensity of each band, and these values, expressed in arbitrary units (A.U.), were normalized by Ponceau-S staining intensity. The results were analyzed using the Student's t-test. PEPT1, MTTP and L-FABP were subjected to the non-parametric test, and all the other proteins were evaluated using the parametric test. The p values of statistically significant results are presented above the bars of the graph; non-significant (NS) data are also indicated. The nitrocellulose membrane was cut at the level of the target proteins using a standard molecular marker as guide. The full area of the selected blots is shown in supplementary data 2.

MTTP (Fig. 5, Panel G) proteins remained unchanged.

3.4. Temporal analysis of nutrient transporter content in mice fed a HFD

To characterize exactly when the alterations in the intestinal protein content begin becoming perturbed by the HFD, the body weights of HFD and LFD mice were measured and protein expression levels were quantified, from 0-12 weeks. As shown in Fig. 6, Panel A, the temporal body weight analysis, over 12 weeks, demonstrated that the LFD mice (black line) displayed a significant increase in body weight gain from the 9th up to 12th week of the experimental protocol, while the HFD mice (red line) presented significant increase in body weight from the 6th up to the 12th week.

Previously, it was shown that the HFD induces a decrease in the expression of GLUT2, PEPT1 and NPC1L1, which was accompanied by an increase in NHE3 content, after consuming the HFD for 12 weeks. Thus, to better understand when these change occur, the protein content of GLUT2, PEPT1, NHE3 and NPC1L1 were evaluated at 3, 6 and 9 weeks into the HFD experimental protocol. It was found that significant reductions in the content of GLUT2 (Fig. 6, Panel B), PEPT1 (Fig. 6, Panel C) and NPC1L1 (Fig. 6, Panel E) were detected in the 3rd week of the HFD protocol, and remained reduced 6 and 9 weeks after HFD initiation. Furthermore, the levels of NHE3 were found to be increased in the 3rd week of the HFD protocol, and remained elevated 6 and 9 weeks after HFD initiation (Fig. 6, Panel D).

4. Discussion

The results of the present study demonstrate that the HFD has the potential of modulating the protein expression levels of nutrient transporters in mice, in as little as three weeks. For example, we observed a downregulated GLUT2, PEPT1, FAT/CD36 and NPC1L1 and upregulated NHE3, MTTP and L-FABP protein expression in the small intestines of mice fed an HFD. It is plausible that NPC1L1, MTTP and L-FABP are transcriptionally regulated, while the altered expression patterns of the other proteins appear to be due to impairments in PKA and/or PKC intracellular signaling pathways. Moreover, obesity, itself, cannot account for the observed modulation of transporter expression levels, since this regulation was not observed in Ob/Ob mice fed a standard chow diet. Thus, reinforcing the notion that the high levels of fat induces these changes in the murine GI tract.

Firstly, we evaluated the content of carbohydrates, peptide and lipid transporters in the small intestine of mice fed an HFD, and detected significant decreases in the content of GLUT2, PEPT1, FAT/CD36 and NPC1L1. Furthermore, that was a concomitant increase in NHE3 content that was detected at 3 weeks, and remained elevated throughout the 12-week HFD-induced obesity protocol. This latter result is consistent with what was previously described in hypo- and hyperthyroid mice fed an HFD for 16 weeks [4]. Additionally, previous work has also shown that mice fed an HFD, for 2 months, also displayed a reduction in GLUT2 and PEPT1 content [31]. These two studies, along with the present results, indicate that high fat intake can effectively modulate the content of glucose and peptides transporters in the small intestine. As a consequence of the downregulated transporter expression, nutrient uptake would be impaired, resulting in fewer nutrients being absorbed. As mentioned previously, these alterations in protein content were detected in the 3rd week after commencing the HFD, thus indicating that these changes were manifested before the establishment of the obesity phenotype, which occurred after 6 weeks of the HFD. These results led to the hypothesis that decreased nutrient transporter expression may attenuate the
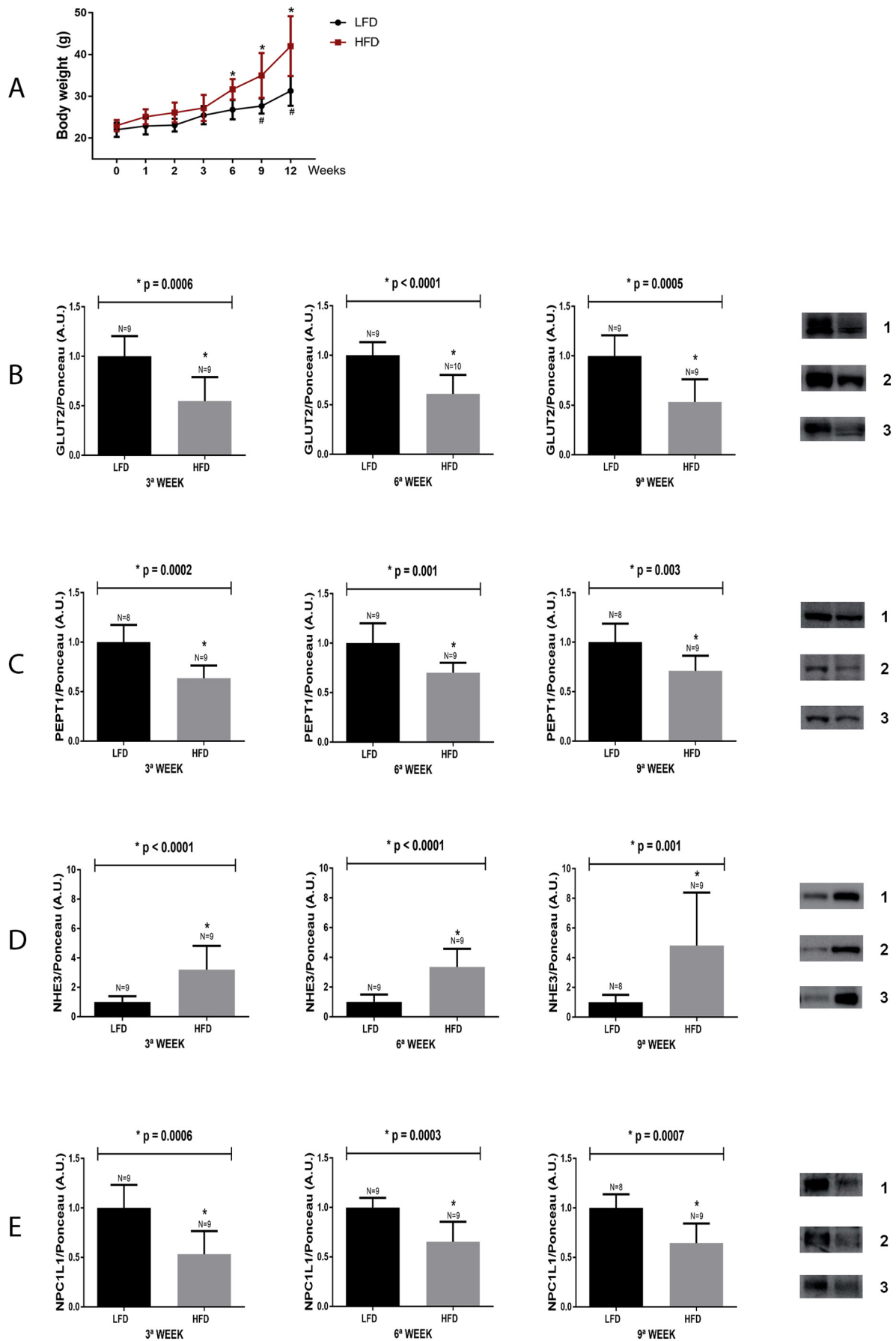
(caption on next page)

Fig. 6. Body weight gain and temporal analysis of nutrient transporter expression in the small intestine of mice fed a LFD or HFD. A: Body weights of mice fed either LFD or HFD were recorded at 1, 2, 3, 6, 9 and 12 weeks after starting the specific diet. Data are from two independent experiments totaling 9 to 10 mice/group. Mice from both groups were euthanized at the 3rd, 6th and 9th week, following diet initiation. The intestinal epithelium was removed, homogenized and processed for detecting the following proteins: B: GLUT2, C: PEPT1, D: NHE3, E: NPC1L1. Representative blots are displayed to the right of the graphs: 1 = 3rd week, 2 = 6th week and 3 = 9th weeks. The number of animals analyzed for each group (N) is also displayed above each bar. Densitometry was used to measure the intensity of each band, and these values, expressed in arbitrary units (A.U.), were normalized by Ponceau-S staining intensity. The p values of statistically significant results are presented above the bars of the graph; non-significant (NS) data are also indicated. The data obtained for body weight,*p < 0.05 *vs* 0 week HFD. #p < 0.05 *vs* 0 week LFD. The nitrocellulose membrane was cut at the level of the target proteins using a standard molecular marker as guide. The full area of the selected blots is shown in supplementary data 2.

progression of obesity, by acting as negative feedback mechanism for body weight maintenance.

With regards to PEPT1, a previous study reported that mice fed an HFD exhibited reduced [^{3}H] Gly-Sar transport, reflecting low PEPT1 activity [32]. Indeed, it is plausible that this observed decrease in activity could be the consequence of the diminished PEPT1 content observed in the mice fed an HFD. Additionally, mice lacking intestinal PEPT1 and fed an HFD displayed reduced body weight and body fat stores, as well as increased energy content in feces, which indicated that the absorption of the dietary constituents in the small intestine was limited [33], and provided support in favor of impaired nutrient uptake in these HFD-induced obese mice.

Additionally, a previous study reported the upregulation of *Mttp* and *L-Fabp* transcripts in the intestines of hamsters fed an HFD [34], which we also observed in the small intestine of obese mice, and it is likely that this transcriptional regulation affects protein expression levels in the cell. In fact, the results presented herein demonstrated that high fat intake enhanced MTTP protein content in the mouse intestine, and is also in accordance with the findings of Chiu et al., which showed an increase in MTTP protein content in the intestine of rats fed an HFD [35]. Furthermore, we also demonstrated an enhancement in the levels of L-FABP in the jejunum, which is the part of the small intestine that expresses the highest L-FABP levels, when compared to the duodenum, ileum and colon [36]. The augmented L-FABP and MTTP protein levels may be a consequence of enhanced gene expression and could also lead to increased chylomicron secretion into the lymphatic vessels. This is due to the fact that following fatty acid absorption, the fatty acids are taken up by endoplasmic reticulum, through the action of L-FABP, re-esterified, and transferred to the nascent chylomicron particles, by MTTP; thus, promoting maturation and increasing the levels of chylomicrons to be secreted [8, 9]. Moreover, the amount of chylomicrons secreted into the lymph vessels is proportional to the levels in the bloodstream, which could lead to dyslipidemia and the comorbidities associated with it [37]. Therefore, the high L-FABP and MTTP levels in the small intestine of mice fed HFD could explain, at least in part, the high prevalence of dyslipidemia presented by obese mice and humans. This is further supported by the fact that the absence of MTTP results in low serum triacylglycerol levels [38].

There is a plethora of studies that have shown that an HFD induces obesity, which, in turn, may trigger several metabolic and cardiovascular disorders. Thus, it was hypothesized that obesity, itself, and not high fat intake, is responsible for the observed alterations in the content of nutrient transporters in the intestines of mice fed an HFD. However, this hypothesis was not entirely supported by the obtained data, since some of these effects were recapitulated in obese Ob/Ob mice, including reduced FAT/CD36 and NPC1L1 protein levels. Therefore, it is plausible that the protein alterations detected in the small intestine of mice fed the HFD were a consequence of high fat content in the digestive tube, ultimately leading to high fat levels in the enterocyte [5], which could possibly influence enterocyte physiology.

In attempt to elucidate a possible mechanism for the observed changes in nutrient transporter expression in enterocytes, the classical components of PKA- and PKC-mediated intracellular signaling were investigated. The HFD group presented low PKA and PKC activities in the small intestine. Such an effect could perturb enterocyte physiology, since it has been shown that PKC stimulates GLUT2 insertion into the enterocyte plasma membrane of rats [39] and can also enhance PEPT1 activity [40]. Thus, suggesting that low PKC activity may be responsible for the reduced GLUT2 and PEPT1 content in mice fed an HFD. However, PEPT1 only possesses PKC phosphorylation sites, and none for PKA. Thus, at least for PEPT1 regulation, the involvement of PKA can be excluded [40].

On the other hand, it is well-established that the function of NHE3 is negatively regulated by PKA [41]. This is consistent with the results presented herein, which showed that NHE3 protein levels were increased, and that PKA activity was significantly decreased in the intestine of mice fed an HFD. In fact, this observation could, at least partially, explain the pathophysiology of hypertension induced by obesity. For example, elevated NHE3 content leads to increased sodium absorption and, consequently, the number of osmotic solutes and water in the bloodstream [42]. Although intestinal NHE3 content of HFD mice remained unchanged 24 h after H89 administration, the link between low PKA activity and NHE3 cannot be discarded, since it has been shown that PKA activation reduces NHE3 activity without altering the NHE3 protein abundance in the plasma membrane [43].

With regards to lipid metabolism, the expression of NPC1L1 did not appear to be modulated by either PKA or PKC, since the H89 administration did not have any effect on NPC1L1 content. Furthermore, it was reported that PKA and PKC analogues do not affect NPC1L1-dependent cholesterol uptake in a rat hepatoma cell line [44]. However, there was an observed decrease in the amount of *Npc1l1* mRNA suggesting that the low intestinal NPC1L1 protein levels are due to a downregulation in *Npc1l1* transcription.
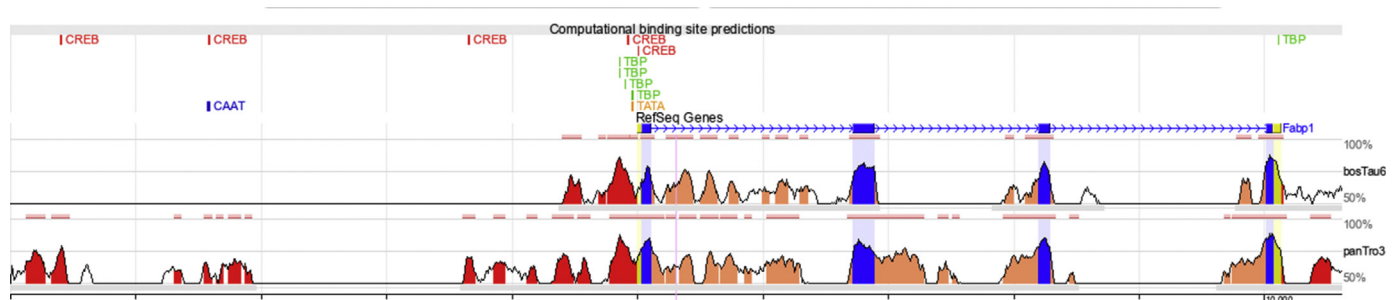

Fig. 7. *In silico* analysis: Computational binding site predictions for CREB, TBP, TATA and CAAT transcription factors on conserved regions located 5 kb upstream of the transcription start site of mouse, chimpanzee and cow *L-Fabp*.

In contrast, the H89 administration reduced FAT/CD36 protein content, which mimicked the effect HFD had on FAT/CD36 levels, and indicates that FAT/CD36 is a target of PKA. Therefore, low PKA activity leads to attenuated FAT/CD36 levels, as evidenced in the intestines of mice fed an HFD. With respect to MTTP protein content, which was increased in the HFD group, there were no detectable changes observed following H89 administration, suggesting that PKA does not play a role in the upregulation of MTTP protein expression in the intestine of mice fed an HFD. As shown, L-FABP content was increased in animals fed an HFD, and this effect was not mimicked by H89 administration. In fact, the levels of this protein were decreased in the intestine, and indicate that another factor, probably related to the PKA signaling pathway, is being recruited. Indeed, total and phosphorylated CREB levels were found to be increased in the HFD group, possibly in response to fatty acid activation [45, 46]. In addition, blocking PKA signaling with H89 reduced the pCREB levels and L-FABP content, which suggests that L-FABP is a gene target of pCREB, acting through a PKA-independent mechanism. Indeed, a preliminary *in silico* analysis identified five binding sites for CREB, 5 kb upstream from the promoter region of the *L-Fabp* gene (Fig. 7).

5. Conclusion

In summary, we showed that mice fed an HFD displayed altered enterocyte physiology, resulting from modulated levels of carbohydrate, peptide and lipid transporters. As a consequence, nutrient absorption is expected to be impaired. The results also provide evidence that elevated NHE3 levels in the intestine could impact sodium absorption, thus representing a possible mechanism for hypertension, which is commonly observed in obese animals, as well as humans. Furthermore, the augmented MTTP and L-FABP levels might be related to enhanced chylomicron secretion, thereby providing a plausible explanation for the observed dyslipidemia associated with obesity. Taken together, all of the identified alterations may be the result of decreased PKA/PKC activity and/or increased pCREB levels.

Declarations

Author contribution statement

Andressa Harumi Hijo, Camille Coutinho, Tatiana Carolina Alba-Loureiro, Jaqueline Santos Moreira Leite: Performed the experiments.

Paula Bargi-Souza: Analyzed and interpreted the data; Wrote the paper.

Francemilson Goulart-Silva: Conceived and designed the experiments; Performed the experiments; Analyzed and interpreted the data; Wrote the paper.

Competing interest statement

The authors declare no conflict of interest.

Additional information

Supplementary content related to this article has been published online at https://doi.org/10.1016/j.heliyon.2019.e02611.

References

[1] T. Yoshikawa, R. Inoue, M. Matsumoto, T. Yajima, K. Ushida, T. Iwanaga, Comparative expression of hexose transporters (SGLT1, GLUT1, GLUT2 and GLUT5) throughout the mouse gastrointestinal tract, Histochem. Cell Biol. 135 (2011) 183–194.

[2] C. Watanabe, Y. Kato, S. Ito, Y. Kubo, Y. Sai, A. Tsuji, Na+/H+ exchanger 3 affects transport property of H+/oligopeptide transporter 1, Drug Metab. Pharmacokinet. 20 (2005) 443–451.

[3] N.A. Abumrad, N.O. Davidson, Role of the gut in lipid homeostasis, Physiol. Rev. 92 (2012) 1061–1085.

[4] M.C. Losacco, C.F.T. de Almeida, A.H.T. Hijo, P. Bargi-Souza, P. Gama, M.T. Nunes, F. Goulart-Silva, High-fat diet affects gut nutrients transporters in hypo and hyperthyroid mice by PPAR-a independent mechanism, Life Sci. 202 (2018) 35–43.

[5] A. Uchida, M.N. Slipchenko, J.X. Cheng, K.K. Buhman, Fenofibrate, a peroxisome proliferator-activated receptor α agonist, alters triglyceride metabolism in enterocytes of mice, Biochim. Biophys. Acta 1811 (2011) 170–176.

[6] X.L. Zhou, B.B. Yan, Y. Xiao, Y.M. Zhou, T.Y. Liu, Tartary buckwheat protein prevented dyslipidemia in high-fat diet-fed mice associated with gut microbiota changes, Food Chem. Toxicol. 119 (2018) 296–301.

[7] M.Y. Park, M.K. Sung, Carnosic acid attenuates obesity-induced glucose intolerance and hepatic fat accumulation by modulating genes of lipid metabolism in C57BL/6J-ob/ob mice, J. Sci. Food Agric. 95 (2015) 828–835.

[8] B.P. Atshaves, G.G. Martin, H.A. Hostetler, A.L. Mclntosh, A.B. Kier, F. Schroeder, Liver fatty acid-binding protein and obesity, J. Nutr. Biochem. 21 (2010) 1015–1032.

[9] M.M. Hussain, P. Rava, M. Walsh, M. Rana, J. Iqbal, Multiple functions of microsomal triglyceride transfer protein, Nutr. Metab. 9 (2012) 14.

[10] J.R. Burnett, G.F. Watts, MTP inhibition as a treatment for dyslipidaemias: time to deliver or empty promises? Expert Opin. Ther. Targets 11 (2007) 181–189.

[11] X. Chang, H. Yan, J. Fei, M. Jiang, H. Zhu, D. Lu, X. Gao, Berberine reduces methylation of the MTTP promoter and alleviates fatty liver induced by a high-fat diet in rats, J. Lipid Res. 51 (2010) 2504–2515.

[12] R.S. Sharma, D.J. Harrison, D. Kisielewski, D.M. Cassidy, A.D. McNeilly, J.R. Gallagher, S.V. Walsh, T. Honda, R.J. McCrimmon, A.T. Dinkova-Kostova, M.L.J. Ashford, J.F. Dillon, J.D. Hayes, Experimental nonalcoholic steatohepatitis and liver fibrosis are ameliorated by pharmacologic activation of Nrf2 (NF-E2 p45-related factor 2), Cell Mol. Gastroenterol. Hepatol. 5 (2017) 367–398.

[13] Y.F. Xing, Z. Zhang, W.J. Fu, D.Q. Zhou, A.C. Yuen, D.K. Mok, C.O. Chan, G.D. Tong, Shugan xiaozhi decoction attenuates nonalcoholic steatohepatitis by enhancing PPARα and L-FABP expressions in high-fat-fed rats, Evid. Based Complement Alternat. Med. (2016).

[14] D. Zhang, Y. Yan, H. Tian, G. Jiang, X. Li, W. Liu, Resveratrol supplementation improves lipid and glucose metabolism in high-fat diet-fed blunt snout bream, Fish Physiol. Biochem. 44 (2018) 163–173.

[15] Y. Zhao, R. Sedighi, P. Wang, H. Chen, Y. Zhu, S. Sang, Carnosic acid as a major bioactive component in rosemary extract ameliorates high-fat-diet-induced obesity and metabolic syndrome in mice, J. Agric. Food Chem. 63 (2015) 4843–4852.

[16] M. Margalit, Z. Shalev, O. Pappo, M. Sklair-Levy, M. Gomori, D. Engelhardt, E. Rabbani, Y. Ilan, Glucocerebroside ameliorates the metabolic syndrome in OB/OB mice, J. Pharmacol. Exp. Ther. 319 (2006) 105–110.

[17] A.J. Kennedy, K.L. Ellacott, V.L. King, A.H. Hasty, Mouse models of the metabolic syndrome, Dis. Model Mech. 3 (2010) 156–166.

[18] E. London, M. Nesterova, C.A. Stratakis, Acute vs chronic exposure to high fat diet leads to distinct regulation of PKA, J. Mol. Endocrinol. 59 (2017) 1–12.

[19] K. Ko, J. Woo, J.Y. Bae, H.T. Roh, Y.H. Lee, K.O. Shin, Exercise training improves intramuscular triglyceride lipolysis sensitivity in high-fat diet induced obese mice, Lipids Health Dis. 17 (2018) 81.

[20] D. Yu, G. Chen, M. Pan, J. Zhang, W. He, Y. Liu, X. Nian, L. Sheng, B. Xu, High fat diet-induced oxidative stress blocks hepatocyte nuclear factor 4α and leads to hepatic steatosis in mice, J. Cell. Physiol. 233 (2018) 4770–4782.

[21] T. Belchior, V.A. Paschoal, J. Magdalon, P. Chimin, T.M. Farias, A.B. Chaves-Filho, R. Gorjão, P. St-Pierre, S. Miyamoto, J.X. Kang, Y. Deshaies, A. Marette, W. Festuccia, Omega-3 fatty acids protect from diet-induced obesity, glucose intolerance, and adipose tissue inflammation through PPARγ-dependent and PPARγ-independent actions, Mol. Nutr. Food Res. 59 (2015) 957–967.

[22] T.E. Oliveira, É. Castro, T. Belchior, M.L. Andrade, A.B. Chaves-Filho, A.S. Peixoto, M.F. Moreno, M. Ortiz-Silva, R.J. Moreira, A. Inague, M.Y. Yoshinaga, S. Miyamoto, N. Moustaid-Moussa, W.T. Festuccia, Fish oil protects wild type and uncoupling protein 1-deficient mice from obesity and glucose intolerance by increasing energy expenditure, Mol. Nutr. Food Res. (2019).

[23] Y. Ye, K.T. Keyes, C. Zhang, J.R. Perez-Polo, Y. Lin, Y. Birnbaum, The myocardial infarct size-limiting effect of sitagliptin is PKA-dependent, whereas the protective effect of pioglitazone is partially dependent on PKA, Am. J. Physiol. Heart Circ. Physiol. 298 (2010) H1454–H1465.

[24] G. Dalmasso, H.T. Nguyen, Y. Yan, H. Laroui, M.A. Charania, T.S. Obertone, S.V. Sitaraman, D. Merlin, MicroRNA-92b regulates expression of the oligopeptide transporter PepT1 in intestinal epithelial cells, Am. J. Physiol. Gastrointest. Liver Physiol. 300 (2011) G52–G59.

[25] M.M. Bradford, A rapid and sensitive method for the quantitation of microgram quantities of protein utilizing the principle of protein-dye binding, Anal. Biochem. 72 (1976) 248–252.

[26] I. Romero-Calvo, B. Ocón, P. Martínez-Moya, M.D. Suárez, A. Zarzuelo, O. Martínez-augustín, F.S. de Medina, Reversible Ponceau staining as a loading control alternative to actin in Western blots, Anal. Biochem. 401 (2010) 318–320.

[27] K.J. Livak, T.D. Schmittgen, Analysis of relative gene expression data using real-time quantitative PCR and the 2(-Delta Delta C(T)) Method, Methods (San Diego, Calif) 25 (2001) 402–408.

[28] A.A. Dussault, M. Pouliot, Rapid and simple comparison of messenger RNA levels using real-time PCR, Biol. Proced. Online 8 (2006) 1–10.

[29] S. Fleige, M.W. Pfaffl, RNA integrity and the effect on the real-time qRT-PCR performance, Mol. Asp. Med. 27 (2006) 126–139.

[30] M.W. Pfaffl, A new mathematical model for relative quantification in real-time RT-PCR, Nucleic Acids Res. 29 (2001) e45.

[31] J.R. Wisniewski, A. Friedrich, T. Keller, M. Mann, H. Koepsell, The impact of high-fat diet on metabolism and immune defense in small intestine mucosa, J. Proteome Res. 14 (2015) 353–365.

[32] P. Hindlet, C. Barraud, L. Boschat, R. Farinotti, A. Bado, M. Buyse, Rosiglitazone and metformin have opposite effects on intestinal absorption of oligopeptides via the proton-dependent PepT1 transporter, Mol. Pharmacol. 81 (2012) 319–327.

[33] D. Kolodziejczak, B. Spanier, R. Pais, J. Kraiczy, T. Stelzl, K. Gedrich, C. Scherling, T. Zietek, H. Daniel, Mice lacking the intestinal peptide transporter display reduced energy intake and a subtle maldigestion/malabsorption that protects them from diet-induced obesity, Am. J. Physiol. Gastrointest. Liver Physiol. 304 (2013) G897–907.

[34] M.C. Lin, C. Arbeeny, K. Bergquist, B. Kienzle, D.A. Gordon, J.R. Wetterau, Cloning and regulation of hamster microsomal triglyceride transfer protein. The regulation is independent from that of other hepatic and intestinal proteins which participate in the transport of fatty acids and triglycerides, J. Biol. Chem. 269 (1994) 29138–29145.

[35] C.Y. Chiu, L.P. Wang, S.H. Liu, M.T. Chiang, Fish oil supplementation alleviates the altered lipid homeostasis in blood, liver, and adipose tissues in high-fat diet-fed rats, J. Agric. Food Chem. 66 (2018) 4118–4128.

[36] Y. Sakai, [Quantitative measurement of liver fatty acid binding protein in human gastrointestinal tract], Nihon Shokakibyo Gakkai Zasshi 87 (1990) 2594–2604.

[37] S. Dash, C. Xiao, C. Morgantini, G.F. Lewis, New insights into the regulation of chylomicron production, Annu. Rev. Nutr. 35 (2015) 265–294.

[38] R.E. Gregg, J.R. Wetterau, The molecular basis of abetalipoproteinemia, Curr. Opin. Lipidol. 5 (1994) 81–86.

[39] G.L. Kellett, The facilitated component of intestinal glucose absorption, J. Physiol. 531 (2001) 585–595.

[40] H.Q. Chen, T.Y. Shen, Y.K. Zhou, M. Zhang, Z.X. Chu, X.M. Hang, H.L. Qin, Lactobacillus plantarum consumption increases PepT1-mediated amino acid absorption by enhancing protein kinase C activity in spontaneously colitic mice, J. Nutr. 140 (2010) 2201–2206.

[41] R.O. Crajoinas, J.Z. Polidoro, C.P. Carneiro de Morais, R.C. Castelo-Branco, A.C. Girardi, Angiotensin II counteracts the effects of cAMP/PKA on NHE3 activity and phosphorylation in proximal tubule cells, Am. J. Physiol. Cell Physiol. 311 (2016) C768–C776.

[42] J.A. Dominguez Rieg, S. de la Mora Chavez, T. Rieg, Novel developments in differentiating the role of renal and intestinal sodium hydrogen exchanger 3, Am. J. Physiol. Regul. Integr. Comp. Physiol. 311 (2016) R1186–R1191.

[43] O.W. Moe, M. Amemiya, Y. Yamaji, Activation of protein kinase A acutely inhibits and phosphorylates Na/H exchanger NHE-3, J. Clin. Investig. 96 (1995) 2187–2194.

[44] J.M. Brown, L.L. Rudel, L. Yu, NPC1L1 (Niemann-Pick C1-like 1) mediates sterol-specific unidirectional transport of non-esterified cholesterol in McArdle-RH7777 hepatoma cells, Biochem. J. 406 (2007) 273–283.

[45] M. Zamarbide, I. Etayo-Labiano, A. Ricobaraza, E. Martínez-Pinilla, M.S. Aymerich, J. Luis Lanciego, A. Pérez-Mediavilla, R. Franco, GPR40 activation leads to CREB and ERK phosphorylation in primary cultures of neurons from the mouse CNS and in human neuroblastoma cells, Hippocampus 24 (2014) 733–739.

[46] I.E. Schauer, J.E. Reusch, Nonesterified fatty acid exposure activates protective and mitogenic pathways in vascular smooth muscle cells by alternate signaling pathways, Metabolism 58 (2009) 319–327.